Indoor Altitude Estimation of Unmanned Aerial Vehicles Using a Bank of Kalman Filters

Conference Paper · May 2020

DOI: 10.1109/ICASSP40776.2020.9054203

6 authors, including:

Liu Yang
Stanford Medicine
16 PUBLICATIONS **119** CITATIONS
SEE PROFILE

Hechuan Wang
Stony Brook University
8 PUBLICATIONS **14** CITATIONS
SEE PROFILE

Yousef El-Laham
Stony Brook University
22 PUBLICATIONS **148** CITATIONS
SEE PROFILE

Mónica F. Bugallo
Stony Brook University
144 PUBLICATIONS **2,174** CITATIONS
SEE PROFILE

INDOOR ALTITUDE ESTIMATION OF UNMANNED AERIAL VEHICLES USING A BANK OF KALMAN FILTERS

Liu Yang[⋆] *Hechuan Wang*[⋆] *Yousef El-Laham*[⋆]
José Ignacio Lamas Fonte[◇] *David Trillo Pérez*[◇] *Mónica F. Bugallo*[⋆]

[⋆]Department of Electrical Engineering, Stony Brook University, Stony Brook, NY (USA)
[◇]Avansig S. L., A Coruña (Spain)
[⋆]{liu.yang.2, hechuan.wang, yousef.ellaham, monica.bugallo}@stonybrook.edu
[◇]{jilamas, dtrillo}@avansig.com

ABSTRACT

Altitude estimation is important for successful control and navigation of unmanned aerial vehicles (UAVs). UAVs do not have indoor access to GPS signals and can only use on-board sensors for reliable estimation of altitude. Unfortunately, most existing navigation schemes are not robust to the presence of abnormal obstructions above and below the UAV. In this work, we propose a novel strategy for tackling the altitude estimation problem that utilizes multiple model adaptive estimation (MMAE), where the candidate models correspond to four scenarios: no obstacles above and below the UAV; obstacles above the UAV; obstacles below the UAV; and obstacles above and below the UAV. The principle of Occam's razor ensures that the model that offers the most parsimonious explanation of the sensor data has the most influence in the MMAE algorithm. We validate the proposed scheme on synthetic and real sensor data.

***Index Terms*—** unmanned aerial vehicles, altitude estimation, Kalman filtering, model selection, drones

1. INTRODUCTION

Over the past decade, unmanned aerial vehicles (UAVs) have gained popularity in a wide-range of applications, including search and rescue operations [1], remote sensing [2, 3], inspection [4], and indoor surveillance [5]. Currently, one of the main challenges for the research community is the development of accurate localization algorithms, which are critical for navigation and collision avoidance [6]. In outdoor settings, UAVs have access to GPS signals that, in conjunction with measurements obtained from on-board sensors, can be used to localize the drone. In indoor settings, however, drones either rely on localization equipment that require extra construction (e.g., tags [7], antennas [8], or specially patterned strips or surfaces [9]) or measurements obtained from on-board sensors, such as distance sensors, barometers, accelerometers, laser scanners [10] and cameras [11, 12, 13]. Indoor localization using only on-board sensors is challenging, especially in the presence of obstacles.

Altitude estimation is one of the key challenges for UAVs in indoor settings, due to the presence of obstructions above and below the UAV [14]. A variety of approaches have been proposed in the literature to address the altitude estimation problem. Both the Kalman filter (KF) and the extended Kalman filter (EKF) [15, 16, 17, 18] have been used to estimate the altitude based on fusion of data from multiple sensors. In another work, altitude estimation is achieved by first filtering sensor measurements, and then combining them using a weighting function [19]. Vision-based machine learning approaches to altitude estimation that rely on an on-board camera [20], and/or laser scanner-based methods such as simultaneous localization and mapping (SLAM) methods [21] have also been proposed. Although some of these methods perform well in simple scenarios, there is still the challenge of obtaining reliable altitude estimation when the obstructions above and below the UAV have irregular shape.

In this work, we propose an algorithm that jointly estimates the UAV's altitude and the height of obstructions above and below the UAV using only infrared (IR) sensor data. The method utilizes a multiple model adaptive estimation (MMAE) [22, 23, 24], which employs a bank of Kalman filters that consider four distinct scenarios: no obstacles above and below the UAV; obstacles above the UAV; obstacles below the UAV; and obstacles above and below the UAV. Each of the stated scenarios corresponds to a candidate model in the MMAE, where the difference in models arises in the observation matrices. The principle of Occam's razor [25] ensures the simplest model that explains the sensor data has the most influence on state estimation. Numerical experiments on synthetic and real data show promising results for the proposed scheme in a variety of different scenarios, including those with irregularly shaped obstacles above and below the UAV.

This paper is organized as follows. First, in Section 2, we give a description of the problem. Section 3 provides a novel state-space formulation to the altitude estimation problem. Section 4 details the proposed estimation method. We present numerical experiments in Section 5 and conclude the paper in Section 6.

2. PROBLEM DESCRIPTION

In this work, we focus on solving the altitude estimation problem for UAV operation in an indoor environment. We consider the UAV architecture presented in Fig. 1, where the altitude estimation system has access to measurements from an IR rangefinder, a sonar rangefinder, and an inertial measurement unit (IMU). We assume we only have access to data from two IR sensors pointing above and below the UAV. We consider TeraRanger One IR sensors, which perform measurements at a high sampling frequency (between 200 and 800 Hz) and with a practical range of about 12 meters.

Figure 2 depicts the altitude estimation scenario in the case that the ceiling of the room is flat and level. The black shapes correspond to obstacles on the ceiling and floor, while the blue curve corresponds to the UAV's trajectory. The UAV is equipped with two IR sensors: one pointed in the direction the ceiling and one pointed in the direction of the floor. The sensors are assumed to be aligned in the same position. Our goal is to estimate the true altitude of the

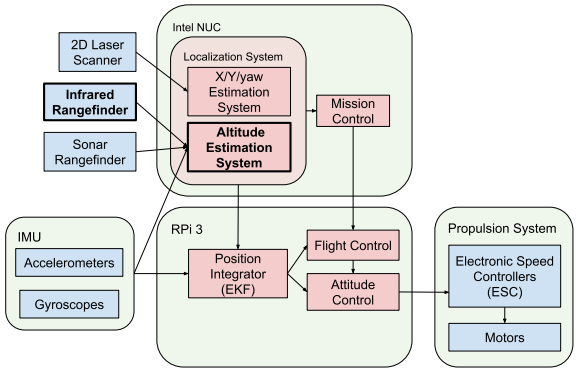

Fig. 1: Considered system architecture.

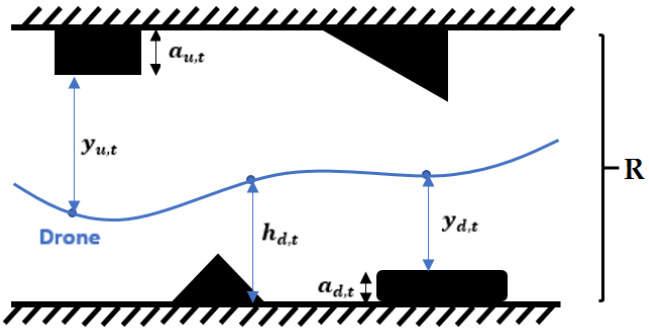

Fig. 2: The altitude estimation scenario.

UAV, denoted by $h_{d,t}$, by measuring the biased range measurements from the upward and downward IR sensors, denoted by $y_{u,t}$ and $y_{d,t}$, under the disturbance of obstacles with the unknown thickness $a_{u,t}$ and $a_{d,t}$. The subscript t denotes time index.

3. STATE-SPACE FORMULATION

In the proposed state-space formulation of the problem, the obstacles above and below the drone are augmented as latent states. Suppose the height of the ceiling R is given. The range measurements from two IR sensors are modeled by the following equations

$$\begin{aligned} y_{u,t} &= R - h_{d,t} - a_{u,t} + \epsilon_{u,t}, \\ y_{d,t} &= h_{d,t} - a_{d,t} + \epsilon_{d,t}, \end{aligned} \tag{1}$$

where $\epsilon_{u,t}, \epsilon_{d,t} \sim \mathcal{N}(0, \sigma_y^2)$ are additive and independent Gaussian observation noises. Rewriting (1) in the matrix form, we have the following observation equation:

$$\mathbf{y}_t = \mathbf{H}\mathbf{x}_t + \boldsymbol{\epsilon}_t, \tag{2}$$

where the vector $\boldsymbol{\epsilon}_t \sim \mathcal{N}(\mathbf{0}, \sigma_y^2 \mathbb{I}_2)$ and $\mathbb{I}_d$ denotes the $d \times d$ identity matrix. The matrix $\mathbf{H}$ is given by

$$\mathbf{H} = \begin{bmatrix} -1 & 0 & -1 & 0 \\ 1 & 0 & 0 & -1 \end{bmatrix}, \tag{3}$$

while the observation vector $\mathbf{y}_t$ and the state vector $\mathbf{x}_t$ are given by

$$\mathbf{y}_t = [y_{u,t} - R, y_{d,t}]^\top \tag{4}$$

$$\mathbf{x}_t = [h_{d,t}, v_t, a_{u,t}, a_{d,t}]^\top \tag{5}$$

where v_t is the vertical velocity of the UAV, which is also regarded as a latent state in this problem.

The state transition equation consists of two parts: one that models how the vertical position of the UAV changes with time, and the other which models our uncertainty about the thickness of obstacles above and below the drone. Let T_s be a known and constant sampling interval. The state transition equations have the following linear form:

$$\begin{aligned} h_{d,t} &= h_{d,t-1} + T_s v_{t-1} + 0.5 T_s^2 u_{v,t-1}, \\ v_t &= v_{t-1} + T_s u_{v,t-1}, \\ a_{u,t} &\sim \mathcal{N}(0, \sigma_a^2), \\ a_{d,t} &\sim \mathcal{N}(0, \sigma_a^2), \end{aligned} \tag{6}$$

where $u_{v,t-1} \sim \mathcal{N}(0, \sigma_v^2)$ denotes the vertical acceleration of the UAV at time $t-1$. The unknown thicknesses $a_{u,t}$ and $a_{d,t}$ of the obstacles are modeled by the i.i.d. zero-mean Gaussian noises, which implies that we do not have any prior information about obstacles at any time. Stacking the equations in (6) together, we can write the transition equation in matrix form:

$$\mathbf{x}_t = \mathbf{F}\mathbf{x}_{t-1} + \mathbf{u}_{t-1} \tag{7}$$

where the state error $\mathbf{u}_{t-1} \sim \mathcal{N}(\mathbf{0}, \mathbf{Q})$ indicates the disturbance on the states of the UAV and our uncertainty about the obstacles. The covariance matrix $\mathbf{Q}$ is given by

$$\mathbf{Q} = \begin{bmatrix} 0.25 T_s^4 \sigma_v^2 & 0.5 T_s^4 \sigma_v^2 & 0 & 0 \\ 0.5 T_s^4 \sigma_v^2 & T_s^4 \sigma_v^2 & 0 & 0 \\ 0 & 0 & \sigma_a^2 & 0 \\ 0 & 0 & 0 & \sigma_a^2 \end{bmatrix}, \tag{8}$$

while the matrix $\mathbf{F}$ is given by

$$\mathbf{F} = \begin{bmatrix} 1 & T_s & 0 & 0 \\ 0 & 1 & 0 & 0 \\ 0 & 0 & 0 & 0 \\ 0 & 0 & 0 & 0 \end{bmatrix}. \tag{9}$$

4. MULTIPLE MODEL ADAPTIVE ESTIMATION

Considering that the state-space model given by (2) and (7) represents the scenario with the obstructions above and below the UAV, we additionally study three simpler models corresponding to the cases where there are no obstacles above and below the UAV, and there are either obstacles above or below the UAV. We use the same state variables $\mathbf{x}_t$ and transition equation (7) in all candidate models and differentiate them only by defining the different observation matrices in (2):

No obstacles: $\mathbf{H}_1 = \begin{bmatrix} -1 & 0 & 0 & 0 \\ 1 & 0 & 0 & 0 \end{bmatrix}$,

Obstacles above: $\mathbf{H}_2 = \begin{bmatrix} -1 & 0 & -1 & 0 \\ 1 & 0 & 0 & 0 \end{bmatrix}$,

Obstacles below: $\mathbf{H}_3 = \begin{bmatrix} -1 & 0 & 0 & 0 \\ 1 & 0 & 0 & -1 \end{bmatrix}$,

Obstacles above and below: $\mathbf{H}_4 = \begin{bmatrix} -1 & 0 & -1 & 0 \\ 1 & 0 & 0 & -1 \end{bmatrix}$,

where $\mathbf{H}_m$ denotes the observability matrix of the mth model for $m = 1, \ldots, 4$. Since all the state-space models are linear and Gaussian, the optimal recursive Bayesian solution with a bank of Kalman filters can be applied to estimate the latent state variables. The proposed MMAE algorithm for altitude estimation is summarized in Table 1 where at each iteration, we conduct Kalman filtering to predict and update the state vectors $\mathbf{x}_{t|t}^{(m)}$ of candidate models, and calculate their marginal likelihoods according to

$$p(\mathbf{y}_{1:t}) = p(\mathbf{y}_{1:t-1})p(\mathbf{y}_t|\mathbf{y}_{1:t-1}) \tag{10}$$

$$= p(\mathbf{y}_{1:t-1}) \int p(\mathbf{y}_t|\mathbf{x}_t)p(\mathbf{x}_t|\mathbf{y}_{1:t-1})d\mathbf{x}_t \tag{11}$$

$$= p(\mathbf{y}_{1:t-1})\mathcal{N}(\mathbf{y}_t|\mathbf{H}\mathbf{x}_{t|t-1}, \mathbf{S}), \tag{12}$$

where $\mathbf{S}$ is the covariance of the innovation. In the practical implementation, the log of the marginal likelihood is usually computed by step 3e in Table 1, where the forgetting factor $\alpha \in [0, 1]$ determines the influence of the observation history in the weighting of the models. The likelihoods are then normalized to determine the weight of each model, which are used to obtain a final estimate of the state vector and error covariance. The principle of Occam's razor states that the simplest model that explains the sensor data well will have the largest weight. We will show the performance of the proposed algorithm, using both synthetic data and real data in the next section.

Algorithm: MMAE for UAV Altitude Estimation

1. **Initialization:** $\mathbf{x}_0, \mathbf{P}_0$
2. **For:** $t = 1, ..., T$
3. **For:** $m = 1, ..., M$

a. Predict the prior state estimate and covariance,

$$\mathbf{x}_{t|t-1}^{(m)} = \mathbf{F}\mathbf{x}_{t-1}$$
$$\mathbf{P}_{t|t-1}^{(m)} = \mathbf{F}\mathbf{P}_{t-1}\mathbf{F}^\top + \mathbf{Q}$$

b. Calculate the innovation and its covariance,

$$\mathbf{z}^{(m)} = \mathbf{y}_t - \mathbf{H}_m\mathbf{x}_{t|t-1}^{(m)}$$
$$\mathbf{S}^{(m)} = \mathbf{H}_m\mathbf{P}_{t|t-1}^{(m)}\mathbf{H}_m^\top + \sigma_y^2\mathbb{I}_2$$

c. Compute the optimal Kalman gain,

$$\mathbf{K}^{(m)} = \mathbf{P}_{t|t-1}^{(m)}\mathbf{H}_m^\top\{\mathbf{S}^{(m)}\}^{-1}$$

d. Update the posterior state estimate and covariance,

$$\mathbf{x}_{t|t}^{(m)} = \mathbf{x}_{t|t-1}^{(m)} + \mathbf{K}^{(m)}\mathbf{z}^{(m)}$$
$$\mathbf{P}_{t|t}^{(m)} = (\mathbb{I}_2 - \mathbf{K}^{(m)}\mathbf{H}_m)\mathbf{P}_{t|t-1}^{(m)}$$

e. Update the log-likelihood of each model,

$$l_{log}^{(m)} = \alpha \times l_{log}^{(m)} - \tfrac{1}{2}\Big[\mathbf{z}^{(m)T}\{\mathbf{S}^{(m)}\}^{-1}\mathbf{z}^{(m)} + \log(|\mathbf{S}^{(m)}|) + 2\log(2\pi)\Big]$$

4. Convert the log-likelihood to the likelihood,

$$l^{(m)} = \exp(l_{log}^{(m)} - \max(l_{log}^{(m)})), m = 1.., M$$

5. Normalize the likelihood,

$$w^{(m)} = l^{(m)} / \textstyle\sum_{i=1}^{M} l^{(i)}, m = 1, ..., M$$

6. Weighted sum the estimates and covariances of models,

$$\mathbf{x}_t = \textstyle\sum_{m=1}^{M} w^{(m)}\mathbf{x}_{t|t}^{(m)}$$
$$\mathbf{P}_t = \textstyle\sum_{m=1}^{M} w^{(m)}\Big[\mathbf{P}_{t|t}^{(m)} + (\mathbf{x}_{t|t}^{(m)} - \mathbf{x}_t)(\mathbf{x}_{t|t}^{(m)} - \mathbf{x}_t)^\top\Big]$$

7. **Return:** $\mathbf{x}_1, \mathbf{x}_2, \ldots, \mathbf{x}_T$.

Note: T is time length and M is the number of models.

Table 1: Applied methodology.

5. EXPERIMENTS

5.1. Synthetic Data

We first apply the proposed method to synthetic data generated from a simulated scenario where regular and irregular obstacles are arranged on the ceiling and floor. Assuming the height of room $R = 3\text{m}$, the sampling interval $T_s = 0.02\text{s}$ and the noise variances $\sigma_v^2 = 0.001\text{m}^2/\text{s}^4$ and $\sigma_y^2 = 0.001\text{m}^2$, we ran 1000 Monte Carlo simulations on the trajectories generated from the initial states $h_{d,0} = 1.5\text{m}$ and $v_0 = 0\text{m/s}$ with $T = 2000$ time length. Note that the constraint $a_{d,t} < h_{d,t} < R - a_{u,t}$ should always be satisfied. The forgetting factor used in the simulations is $\alpha = 0.8$.

We summarize the mean squared errors (MSEs) of the Monte Carlo simulations at different noise levels in Table 2, where we can see that the best performance is achieved when $\sigma_y^2 = 0.001\text{m}^2$, $\sigma_v^2 = 0.1\text{m}^2/\text{s}^4$ and $\sigma_a^2 = 1\text{m}^2$. The variance of vertical acceleration describes the smoothness in the drone flight, while the variance of thickness explains how much uncertainty we have about the obstacles. Figure 3 compares the altitude estimation from MMAE and KF of model 4 for one specific simulation at the best setting of parameters, which demonstrates that the method works well even in the scenario where there are irregular obstacles above and below the UAV. The normalized likelihoods of the models are stacked together in Fig. 5, where we can see that the weights jump between 0 and 1 consistently with the simulation scenario.

σ_y^2	0.001			0.01		
σ_a^2 \ σ_v^2	0.01	0.1	1	0.01	0.1	1
0.01	2.8e-3	4.8e-3	1.3e-2	4.6e-3	6.6e-3	1.4e-2
0.1	1.4e-3	2.4e-4	5.1e-4	1.9e-3	7.3e-4	7.7e-4
1	1.4e-3	**2.3e-4**	2.9e-4	2.1e-3	1.4e-3	2.9e-2

Table 2: MSEs of altitude estimation in synthetic data experiment.

5.2. Real Data

Next, we test the proposed algorithm with the real data[1]. In the experiments, the UAV flies at a fixed altitude $h_{d,t} = 1.7\text{m}$ in a room of $R = 2.88\text{m}$ remaining the same pitch and roll angles during the experiments. The UAV passes over the regular obstacles with parallel or inclined surfaces, such as tables, boxes and ramps, and obstacles of irregular shape. Simultaneously, it flies under the regular and

[1]Real data provided by Avansig S.L.

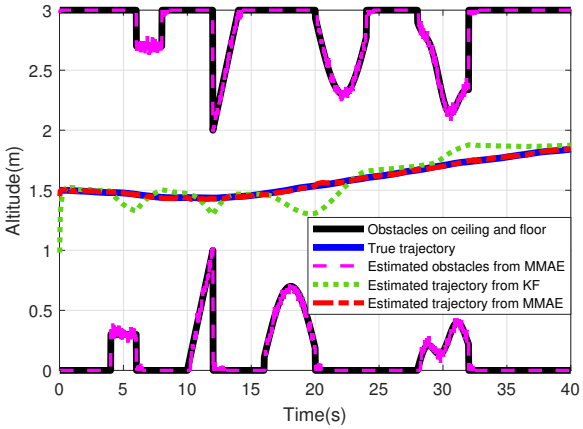

Fig. 3: An altitude estimation result from a simulated scenario.

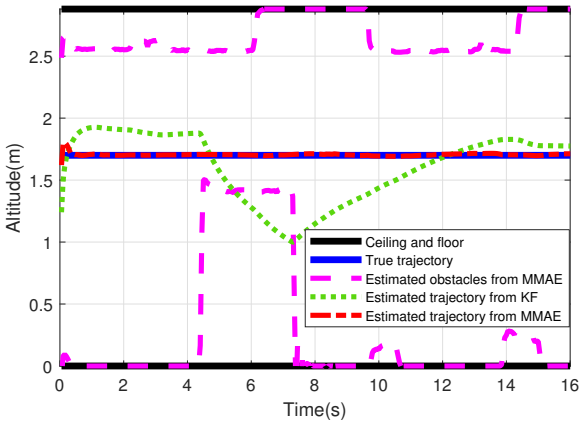

Fig. 4: An altitude estimation result in the practical scenario.

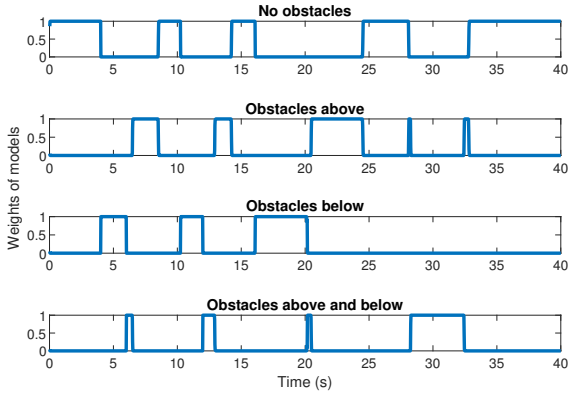

Fig. 5: The corresponding model weights for the result in Fig. 3.

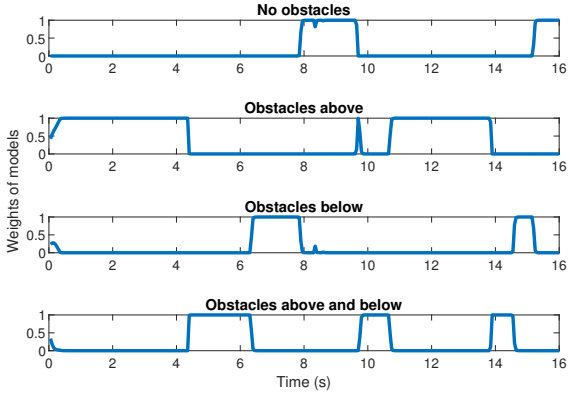

Fig. 6: The corresponding model weights for the result in Fig. 4.

Ceiling \ Floor	None	Regular Parallel	Regular Inclined	Irregular
None	1.36e-4	3.57e-5	9.42e-5	1.49e-4
Regular	2.53e-4	3.61e-4	3.58e-4	4.25e-4
Irregular	4.51e-4	5.93e-4	9.50e-4	5.14e-4

Table 3: MSEs of altitude estimation in real data experiment.

irregular ceiling topology (level changes and light fixtures). The collected data include the range measurements $y_{u,t}$ and $y_{d,t}$ from two IR sensors and the information from the IMU. Based on the available data, the sampling interval is known and is $T_s = 0.05$s. The variance of the vertical acceleration is around $\sigma_v^2 = 0.2\text{m}^2/\text{s}^4$.

We run the proposed method for 12 scenarios corresponding to different arrangements of the obstacles on the ceiling and floor. Based on the *a priori* information and the size of potential obstructions, we selected the variances of observation noise $\sigma_y^2 = 0.001\text{m}^2$ and the uncertainty of obstacles $\sigma_a^2 = 1\text{m}^2$. The forgetting factor used is $\alpha = 0.67$. The MSEs of the altitude estimation from those scenarios are summarized in Table 3. From these results, we can see that the proposed approach performs very well. Figure 4 shows an example where the drone was flying in an indoor environment with regular and irregular obstacles above and below. The estimated trajectory is accurate when compared to the real one and also the one from KF. In addition, the weights of the models are plotted in Fig. 6 and are consistent with the above scenario.

6. CONCLUSION

This paper addressed the problem of altitude estimation for unmanned aerial vehicles (UAV) in an indoor setting. The proposed solution is based on deriving a state-space formulation to the problem, where obstacles are augmented as latent states. The UAV altitude and obstacle states are obtained by applying multiple adaptive model estimation, which uses a bank of four Kalman filters that each consider a distinct observation matrix. Simulations using both synthetic and real data show promise of the proposed approach. Future work will consider more ambitious models that will incorporate measurements from other sensors, such as an ultrasound sensor and an inertial measurement unit.

7. REFERENCES

[1] Y. Karaca, M. Cicek, O. Tatli, A. Sahin, S. Pasli, M. F. Beser, and S. Turedi, "The potential use of unmanned aircraft systems (drones) in mountain search and rescue operations," *The American Journal of Emergency Medicine*, vol. 36, no. 4, pp. 583–588, 2018.

[2] D. Anthony, S. Elbaum, A. Lorenz, and C. Detweiler, "On crop height estimation with UAVs," in *2014 IEEE/RSJ International Conference on Intelligent Robots and Systems*. IEEE, 2014, pp. 4805–4812.

[3] V. V. Klemas, "Coastal and environmental remote sensing from unmanned aerial vehicles: An overview," *Journal of Coastal Research*, vol. 31, no. 5, pp. 1260–1267, 2015.

[4] R. Ashour, T. Taha, F. Mohamed, E. Hableel, Y. A. Kheil, M. Elsalamouny, M. Kadadha, K. Rangan, J. Dias, L. Seneviratne, and G. Cai, "Site inspection drone: A solution for inspecting and regulating construction sites," in *2016 IEEE 59th International Midwest Symposium on Circuits and Systems (MWSCAS)*. IEEE, 2016, pp. 1–4.

[5] K. S. Lee, M. Ovinis, T. Nagarajan, R. Seulin, and O. Morel, "Autonomous patrol and surveillance system using unmanned aerial vehicles," in *2015 IEEE 15th International Conference on Environment and Electrical Engineering (EEEIC)*. IEEE, 2015, pp. 1291–1297.

[6] N. Gageik, P. Benz, and S. Montenegro, "Obstacle detection and collision avoidance for a UAV with complementary low-cost sensors," *IEEE Access*, vol. 3, pp. 599–609, 2015.

[7] T. Sanpechuda and L. Kovavisaruch, "A review of RFID localization: Applications and techniques," in *2008 5th International Conference on Electrical Engineering/Electronics, Computer, Telecommunications and Information Technology*. IEEE, 2008, vol. 2, pp. 769–772.

[8] L. Brás, N. B. Carvalho, P. Pinho, L. Kulas, and K. Nyka, "A review of antennas for indoor positioning systems," *International Journal of Antennas and Propagation*, vol. 2012, 2012.

[9] R. J. Orr and G. D. Abowd, "The smart floor: A mechanism for natural user identification and tracking," in *CHI Extended Abstracts*. ACM, 2000, pp. 275–276.

[10] J. Zhang and S. Singh, "LOAM: Lidar odometry and mapping in real-time.," in *Robotics: Science and Systems*, 2014, vol. 2, p. 9.

[11] A. J. Davison, I. D. Reid, N. D. Molton, and O. Stasse, "MonoSLAM: Real-time single camera SLAM," *IEEE Transactions on Pattern Analysis & Machine Intelligence*, , no. 6, pp. 1052–1067, 2007.

[12] M. Tomono, "Robust 3D SLAM with a stereo camera based on an edge-point ICP algorithm," in *2009 IEEE International Conference on Robotics and Automation*. IEEE, 2009, pp. 4306–4311.

[13] J. Engel, J. Sturm, and D. Cremers, "Camera-based navigation of a low-cost quadrocopter," in *2012 IEEE/RSJ International Conference on Intelligent Robots and Systems*. IEEE, 2012, pp. 2815–2821.

[14] S. Grzonka, G. Grisetti, and W. Burgard, "Towards a navigation system for autonomous indoor flying," in *2009 IEEE International Conference on Robotics and Automation*. IEEE, 2009, pp. 2878–2883.

[15] P. Gąsior, S. Gardecki, J. Gośliński, and W. Giernacki, "Estimation of altitude and vertical velocity for multirotor aerial vehicle using Kalman filter," in *Recent Advances in Automation, Robotics and Measuring Techniques*, pp. 377–385. Springer, 2014.

[16] H. Bavle, J. L. Sanchez-Lopez, A. Rodriguez-Ramos, C. Sampedro, and P. Campoy, "A flight altitude estimator for multirotor UAVs in dynamic and unstructured indoor environments," in *2017 International Conference on Unmanned Aircraft Systems (ICUAS)*. IEEE, 2017, pp. 1044–1051.

[17] W. Chen, Y. Dong, and Z. Duan, "Attacking altitude estimation in drone navigation," in *IEEE INFOCOM 2018-IEEE Conference on Computer Communications Workshops (INFOCOM WKSHPS)*. IEEE, 2018, pp. 888–893.

[18] S. J. Julier and J. K. Uhlmann, "New extension of the Kalman filter to nonlinear systems," in *Signal Processing, Sensor Fusion, and Target Recognition VI*. International Society for Optics and Photonics, 1997, vol. 3068, pp. 182–193.

[19] G. Szafranski, R. Czyba, W. Janusz, and W. Blotnicki, "Altitude estimation for the UAV's applications based on sensors fusion algorithm," in *2013 International Conference on Unmanned Aircraft Systems (ICUAS)*. IEEE, 2013, pp. 508–515.

[20] A. Cherian, J. Andersh, V. Morellas, N. Papanikolopoulos, and B. Mettler, "Autonomous altitude estimation of a UAV using a single onboard camera," in *2009 IEEE/RSJ International Conference on Intelligent Robots and Systems*. IEEE, 2009, pp. 3900–3905.

[21] S. Riisgaard and M. R. Blas, "SLAM for dummies," *A Tutorial Approach to Simultaneous Localization and Mapping*, vol. 22, no. 1-127, pp. 126, 2003.

[22] P. S. Maybeck and P. D. Hanlon, "Performance enhancement of a multiple model adaptive estimator," *IEEE Transactions on Aerospace and Electronic Systems*, vol. 31, no. 4, pp. 1240–1254, 1995.

[23] P. D. Hanlon and P. S. Maybeck, "Multiple-model adaptive estimation using a residual correlation Kalman filter bank," *IEEE Transactions on Aerospace and Electronic Systems*, vol. 36, no. 2, pp. 393–406, 2000.

[24] B. N. Alsuwaidan, J. L. Crassidis, and Y. Cheng, "Generalized multiple-model adaptive estimation using an autocorrelation approach," *IEEE Transactions on Aerospace and Electronic systems*, vol. 47, no. 3, pp. 2138–2152, 2011.

[25] C. E. Rasmussen and Z. Ghahramani, "Occam's razor," in *Advances in Neural Information Processing Systems*, 2001, pp. 294–300.